

# Suppression of $\mu^+$ depolarization by fast magnetic fluctuations at avoided level crossings for $\text{Ho}^{3+}$ ions in $\text{CaWO}_4$

E. Kenney,<sup>1</sup> A. Amato,<sup>2</sup> S. R. Giblin,<sup>3</sup> B. Z. Malkin,<sup>4</sup> and M. J. Graf<sup>1,\*</sup>

<sup>1</sup>*Department of Physics, Boston College, Chestnut Hill, Massachusetts 02467, USA*

<sup>2</sup>*Paul Scherrer Institute, CH 5232 Villigen PSI, Switzerland*

<sup>3</sup>*School of Physics and Astronomy, Cardiff University, Cardiff CF24 3AA, United Kingdom*

<sup>4</sup>*Kazan Federal University, Kremlevskaya 18, Kazan 420008, Russian Federation*



(Received 23 May 2018; revised manuscript received 15 August 2018; published 15 October 2018)

We use transverse field muon spin rotation to probe the low field dynamics of  $\text{Ho}^{3+}$  ions imbedded in a single crystal host matrix of  $\text{CaWO}_4$ . The  $\text{Ho}^{3+}$  ions at sites with the full tetragonal symmetry of the crystal have avoided level crossings of hyperfine sublevels of the ground crystal-field doublet, resulting in measurable changes in the both the AC susceptibility and transverse field muon depolarization rate. The host material has primarily nonmagnetic nuclear species and no magnetic ions, and so the muon is shown to be a direct nonresonant probe of pronounced changes of relaxation rates of the coupled electron-nuclear excitations of  $\text{Ho}^{3+}$  at avoided level crossings.

DOI: [10.1103/PhysRevB.98.134424](https://doi.org/10.1103/PhysRevB.98.134424)

## I. INTRODUCTION

The properties of nearly isolated spins in a solid host are of fundamental interest, exhibiting quantum dynamical phenomena, e.g., tunneling of magnetization [1], and which offer future application potential such as memory storage and quantum computing. The spin dynamics of  $\text{Ho}^{3+}$  ions lightly doped into the tetragonal single crystal host material  $\text{LiYF}_4$  (LYF:Ho) proved to be a useful paradigm system: the high quality and well-characterized host matrix provided a system whereby theoretical modeling based on known physical parameters could be used to describe the spin dynamics observed through magnetization [2], AC susceptibility [3–5], and nuclear magnetic resonance [6,7]. The holmium ions substitute for yttrium trivalent ions at sites with  $S_4$  point symmetry. The lowest multiplet  $^5I_8$  of  $\text{Ho}^{3+}$  ions in the crystal field of tetragonal  $\text{LiYF}_4$  is split into singlets  $\Gamma_1$  and  $\Gamma_2$  and non-Kramers doublets  $\Gamma_{34}$  (the  $\Gamma$ 's are the corresponding irreducible representations of the  $S_4$  group). The ground state is a magnetic doublet ( $g$  factor  $\approx 13$  for fields along the  $c$  axis, and zero in the  $a$ - $b$  plane) separated from the first excited singlet  $\Gamma_2$  by approximately 10 K [2]. Due to the strong hyperfine coupling, the  $I = 7/2$  Ho nucleus further splits this doublet into eight doubly degenerate levels, separated from one another in zero field by approximately 0.22 K. Application of a weak magnetic field  $\mathbf{B}||c$  lifts this degeneracy and results in a sequence of level crossings at fields of  $B_n = 23n$  mT, where  $n$  is an integer and  $-7 \leq n \leq 7$  [2]. The low temperature, low magnetic field spin dynamics are dominated by the presence of fairly large avoided level crossings (ALCs) when  $n$  is odd [2,8], corresponding to transitions between the hyperfine sublevels where the change in the nuclear spin

projections on the symmetry axis ( $z||c$ )  $\Delta I_z = 2$ ; these large tunneling gaps result from mixing of wave functions of the ground state doublet and the first excited singlet by the hyperfine interaction. Smaller random strain-induced gaps are also present at  $\Delta I_z = 0$  crossings at field values corresponding to odd values of  $n$  (see inset in Fig. 1) [9].

Transverse field muon spin rotation ( $\mu$ SR) experiments on LYF:Ho [8] provided an unusual mechanism for probing the change in spin dynamics at these ALCs. Sharp dips were observed in the muon transverse field depolarization rate  $\lambda_{TF}$  at field values corresponding to  $n = 1$  and 3, while a much smaller reduction was observed at  $n = 2$ . It was proposed that the depolarization was due to the nearly static disorder of the  $\text{Ho}^{3+}$  ions; however, near large gaps at ALCs the magnetic fluctuation rate increased significantly, thereby reducing the static disorder on the muon timescale and causing a decrease in  $\lambda_{TF}$ . Given the dilute  $\text{Ho}^{3+}$  ion distribution one outstanding concern is the nature of the muon coupling to the  $\text{Ho}^{3+}$  ions. It is known that the  $^{19}\text{F}$  spin bath strongly couples to the  $\text{Ho}^{3+}$  ions [7], and the  $F^-$  ion strongly interacts with (indeed, *bonds to*) the implanted muons in a  $\mu$ SR experiment [8,10]. The presence of possible multiple muon depolarization channels calls into question the interpretation of the results from Ref. [8], and in particular whether or not the muon is directly probing the magnetic fluctuations of the  $\text{Ho}^{3+}$  ions. As described below, we can experimentally answer this question by removing the  $\mu^+ - F^-$  depolarization channel. Thus, we have a quantifiable method of demonstrating the direct depolarization of the muon by dilute magnetic moments.

In this paper we use transverse field  $\mu$ SR to probe the low field dynamics of  $\text{Ho}^{3+}$  ions imbedded in a single crystal host matrix of Scheelite  $\text{CaWO}_4$  (CWO:Ho). This host is isostructural with  $\text{LiYF}_4$ , and detailed studies via optical and electron paramagnetic resonance (EPR) spectroscopy of CWO:Ho showed that the energy level diagrams of  $\text{Ho}^{3+}$  in both hosts are qualitatively identical [11], although the

\*Author to whom correspondence should be addresses: [grafm@bc.edu](mailto:grafm@bc.edu)

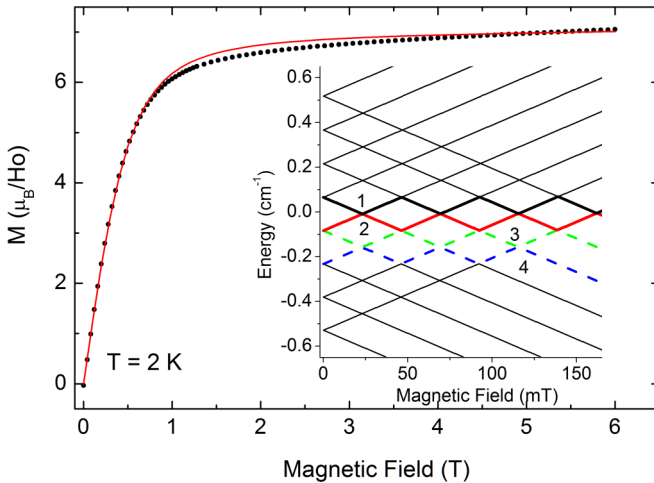


FIG. 1. DC magnetization versus magnetic field directed along the tetragonal symmetry axis, along with the fit (solid line) as described in the text. Inset: Computed magnetic field dependences of the energies of the 16 lowest electron-nuclear states of  $\text{Ho}^{3+}$  ions in tetragonal centers. Points of repulsion between the thick zig-zag lines 1 and 2 and between the dashed lines 3 and 4 correspond to anticrossings with  $\Delta I_z = 0$  and  $\Delta I_z = 2$ , respectively.

heterovalent substitution required to maintain charge balance in CWO:Ho (see below) creates a substantial number of  $\text{Ho}^{3+}$  centers lacking the tetragonal crystal symmetry. There is no electronic contribution to the magnetic properties from the valence electrons of the host matrix, and only very low concentrations of weak nuclear moments associated with the 14%  $^{183}\text{W}$  and substitutional  $^7\text{Li}^+$  impurities (see below), and so in this system there is no intermediary nuclear spin bath. We find very similar results to those presented in Ref. [8], demonstrating that the muon is indeed a direct probe of the  $\text{Ho}^{3+}$  spin dynamics, even when there are multiple possible relaxation channels present as in the case of LYF:Ho.

## II. EXPERIMENTAL DETAILS AND RESULTS

The CWO:Ho sample used in this work, with a nominal Ho concentration of 0.5%, was studied in Ref. [11], and was grown by Czochralski technique from  $\text{Ho}_2\text{O}_3$ ,  $\text{WO}_3$ ,  $\text{CaCO}_3$ , and  $\text{Li}_2\text{CO}_3$ . The  $\text{Ho}^{3+}$  substitutes for  $\text{Ca}^{2+}$ , and charge balance is maintained by  $\text{Li}^+$  replacement of  $\text{Ca}^{2+}$  during growth.

AC susceptibility and DC magnetization measurements were made in a Quantum Design MPMS3 superconducting quantum interference device (SQUID) system. The DC magnetization at 2 K in fields up to 6 T (Fig. 1) showed that the actual Ho concentration in our sample was approximately 0.2%, as described below. The magnetization and AC susceptibility data and the fits shown in Figs. 1 and 2 will be discussed later in this work.

In time-differential  $\mu\text{SR}$ , a spin-polarized  $\mu^+$  enters a sample, and within 10 ps or less it comes to rest, typically at one or two electrostatically favorable crystalline sites. In this paper the specific stopping site is not relevant, given that the muon is

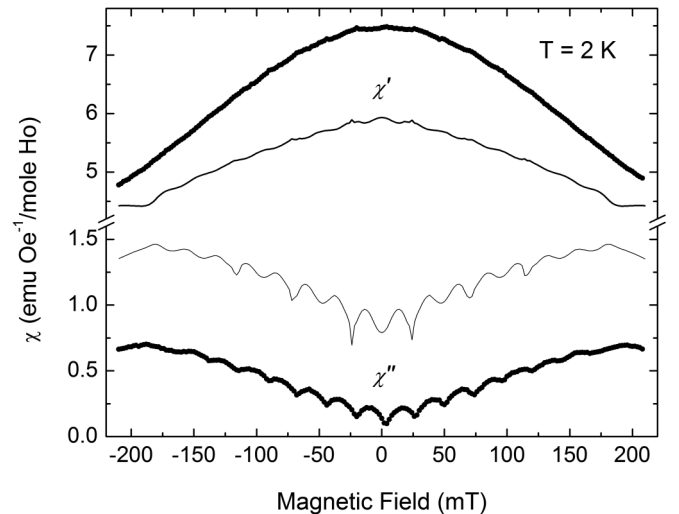


FIG. 2. In-phase ( $\chi'$ ) and out-of-phase ( $\chi''$ ) susceptibility versus magnetic field directed along the tetragonal symmetry axis, taken at a frequency of 953 Hz and with an excitation level of 1.5 Oe. The fine solid lines are simulated results as described in the text.

interacting with dilute magnetic impurities. At some later time  $t$  the muon decays, and the resulting positron is preferentially emitted along the direction of the muon spin moment and detected. After several million decay events one creates a time histogram of the detector signal asymmetry  $A(t)$  [12], which is proportional to the muon polarization and characterizes its response to the local magnetic fields at the muon stopping sites. We assume that the stopping sites as well as the impurity  $\text{Ho}^{3+}$  ions are distributed randomly in the sample volume. In transverse field mode, the initial muon polarization has a component perpendicular to the applied magnetic field  $\mathbf{B}$ , resulting in muon precession. Variations of the local magnetic field between muon stopping sites produce a dephasing of  $A(t)$  due to the spread of Larmor frequencies for the individual muon decay events, and so transverse field measurements are extremely sensitive to magnetic inhomogeneity.

The  $\mu\text{SR}$  measurements were conducted on the General Purpose Spectrometer on the  $\pi\text{M}_3$  continuous beamline at the Paul Scherrer Institute. The beam momentum and external magnetic field were aligned parallel to the crystalline  $c$  axis. Experiments were conducted in a gas flow cryostat and our measurements span the range  $1.6 \text{ K} \leq T \leq 20 \text{ K}$ . We utilized the spin-rotated mode, where the muon spin is tilted approximately  $50^\circ$  with respect to the beam momentum. The transverse field depolarization is then monitored with detectors oriented along a line perpendicular to the applied magnetic field.

In Fig. 2 we show the magnetic field variation of the AC susceptibility at a frequency of 953 Hz and AC amplitude of 1.5 Oe at 2 K; the oscillating magnetic field, as well as the constant field  $\mathbf{B}$ , was oriented along the  $c$  axis. The out-of-phase component  $\chi''$  shows dips at the  $B_n$  values listed above [4,5], while the in-phase component  $\chi'$  has barely discernible peaks at  $B_n$ . We find the minima in  $\chi''$  exhibit an average spacing of roughly 22.9 mT; a comparison with the value of  $B_1 = 23.1 \text{ mT}$  obtained from calculations (see inset in Fig. 1)

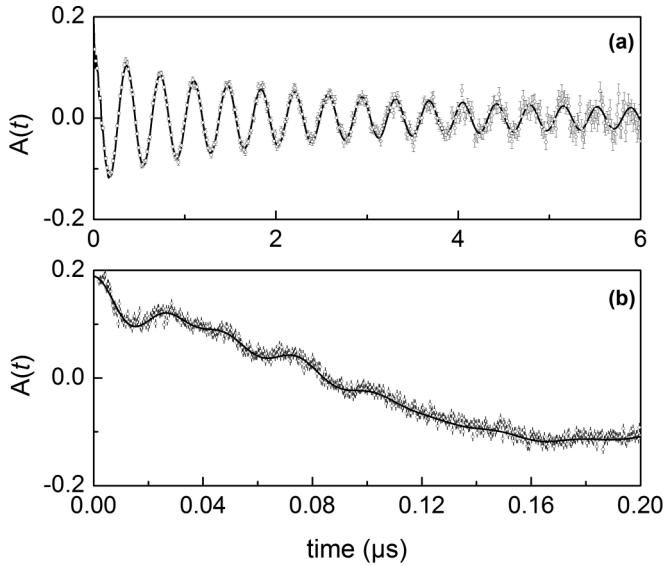


FIG. 3. (a) Depolarization at a temperature  $T = 1.8$  K and in an applied magnetic field of 20 mT. (b) Short-time depolarization for the sum of our signals at 23 mT for temperatures from 1.8 K to 20 K, highlighting the muonium oscillations. The solid lines in both (a) and (b) are the fits to the data, as described in the text.

indicates a misalignment less than  $3^\circ$  of the applied field with the  $c$  axis.

Zero-field muon-spin depolarization versus time data (not shown) were taken at 20 K. A very fast depolarization constituting 25% of the signal was observed, while the remaining signal was essentially constant in time. The fast relaxation originates from the formation of a bound pair  $\mu^+e^-$  (muonium), see also below. We fit the slowly relaxing signal to a simple exponential decay, and find a depolarization rate of  $0.04(1) \mu\text{s}^{-1}$ , confirming the very small contribution of the host matrix to the observed relaxation. In Fig. 3(a) we show the time dependent asymmetry of the muon at  $T = 1.8$  K and in a magnetic field  $\mathbf{B} \parallel \mathbf{c}$  with  $B = 20$  mT. The signal consists of three components: two high frequency oscillatory signals evident at short times, along with a slow oscillation at the expected precession frequency  $f_\mu = 2.71$  MHz which is determined by  $f_\mu = (\gamma_\mu/2\pi)B$ , where  $\gamma_\mu$  is the muon gyromagnetic ratio and  $\gamma_\mu/2\pi = 135.5$  MHz/T. The short time signal was found to be independent of temperature below 20 K, so to accurately characterize it we summed all our data between 1.8 and 20 K, and this sum at short times is shown in Fig. 3(b). The fast oscillations have frequencies of  $28.1(2)$  and  $39.6(3)$  MHz at 20 mT, consistent with muonium formation as reported, for example, for silicon in Ref. [13]. These correspond to the transitions between the muonium triplet states, for which the degeneracy is lifted by the applied magnetic field. So, our overall depolarization function (asymmetry normalized by its value at  $t = 0$ ) was therefore fit to a three-component function

$$P(t) = \sum_{i=1}^3 a_i \exp[-(\lambda_i t)^{\beta_i}] \cos(2\pi f_i t + \phi_i), \quad (1)$$

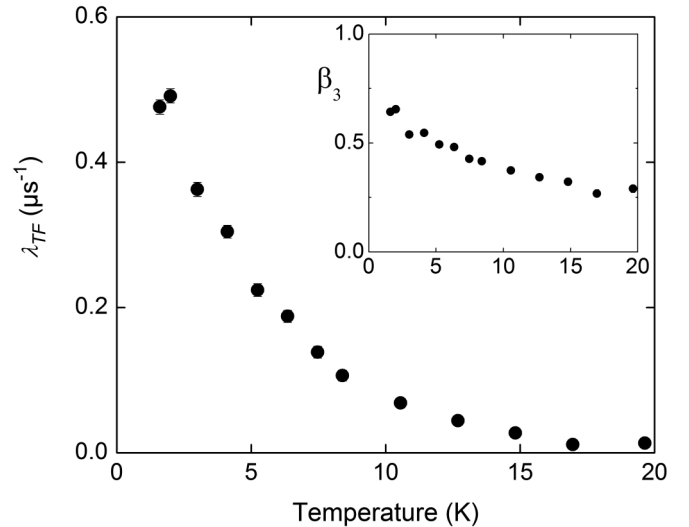


FIG. 4. Temperature dependences of the transverse field depolarization rate in an applied field of 23 mT. Inset: variation of the damping exponent with temperature.

where the first two terms ( $i = 1, 2$ ) are associated with the muonium oscillations, and the third term with the precessing free muon located at an interstitial site in the sample. These fits are shown as solid lines in Figs. 3(a) and 3(b). We found that the  $a_i$  were constant, with  $a_1 = 0.11(1)$ ,  $a_2 = 0.15(1)$ , and  $a_3 = 0.74(3)$ . Assuming constant values  $\beta_1 = \beta_2 = 1$ , we extracted fit values  $\lambda_1 = 13(2) \mu\text{s}^{-1}$  and  $\lambda_2 = 19(3) \mu\text{s}^{-1}$  which were assumed independent of temperature and field. The frequencies  $f_{1,2}$  varied weakly with field (see Fig. 6) as expected for muonium in a low magnetic field. The phases were found to be  $\phi_1 = -31(5)^\circ$ ,  $\phi_2 = -10(5)^\circ$ , and  $\phi_3 = 5.3(1)^\circ$ , and fixed at these values. The muon precession damping coefficient  $\lambda_3 = \lambda_{TF}$  and exponent  $\beta_3$  varied with both field and temperature.

The temperature dependence of  $\lambda_{TF}$  is shown in Fig. 4, along with  $\beta_3$  in the inset. Because the crystal host is non-magnetic, damping is caused primarily by the  $\text{Ho}^{3+}$  ions. Near 20 K, the damping is quite weak and the exponent  $\beta_3$  is roughly  $1/3$ , which we interpret as the motional narrowing limit for thermally induced fluctuations of the  $\text{Ho}^{3+}$  moments [12]. As the temperature is lowered well below 13 K, only the lowest lying energy manifold is occupied and the rate of fluctuations is reduced substantially, with the exponent approaching a value of approximately  $\beta_3 \approx 0.7$ . This is smaller than the value  $\approx 1.2$  for  $\text{Ho}^{3+}$  ions in LYF [8] due to the lack of a contribution from quasistatic fluorine nuclear moments, which would have an expected exponent of 2 [8,12]. This provides further evidence that the muon depolarization is modified solely by magnetism associated with  $\text{Ho}^{3+}$ , without complications from other sources of magnetism.

In Fig. 5 we show our results for the field dependence of  $\lambda_{TF}$  at low temperature ( $T = 1.6$  K), along with  $\beta_3$  in the inset. Away from  $n = 1$  ( $\approx 23$  mT) the background damping due to quasistatic magnetic inhomogeneity of dipolar fields produced by the  $\text{Ho}^{3+}$  ions is  $0.5 \mu\text{s}^{-1}$ , lower than  $0.9 \mu\text{s}^{-1}$  for LYF:Ho. Again, this is reasonably well accounted for by the absence of a contribution from the  $^{19}\text{F}$  nuclei, which

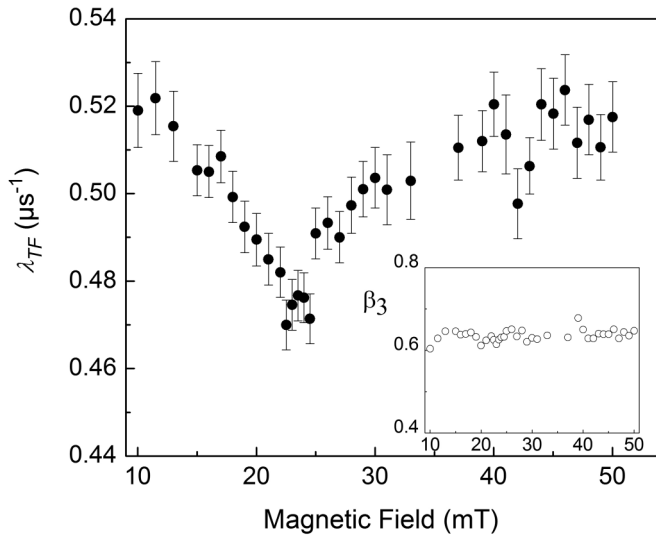


FIG. 5. Field dependence of the transverse field depolarization rate versus magnetic field at a  $T = 1.6$  K. Inset: variation of the damping exponent with magnetic field.

was determined to be  $\approx 0.4 \mu\text{s}^{-1}$  from high temperature measurements [8]. A sharp dip, corresponding to a decrease of roughly 10% of  $\lambda_{TF}$ , is observed near 23 mT, along with a very weak structure near 46 mT, as observed in Ref. [8]. The exponent  $\beta_3$  is nearly field independent. Finally, in Fig. 6 we show the weak magnetic field variation of  $f_1$  and  $f_2$ , which qualitatively agrees with field dependence observed for anomalous muonium in silicon [13].

### III. DISCUSSION

The close similarity of the results obtained for LYF:Ho and CWO:Ho samples shows that the muon is responding directly to changes in rates of the  $\text{Ho}^{3+}$  dipolar magnetic fluctuations at the avoided level crossing  $n = 1$ , and neither

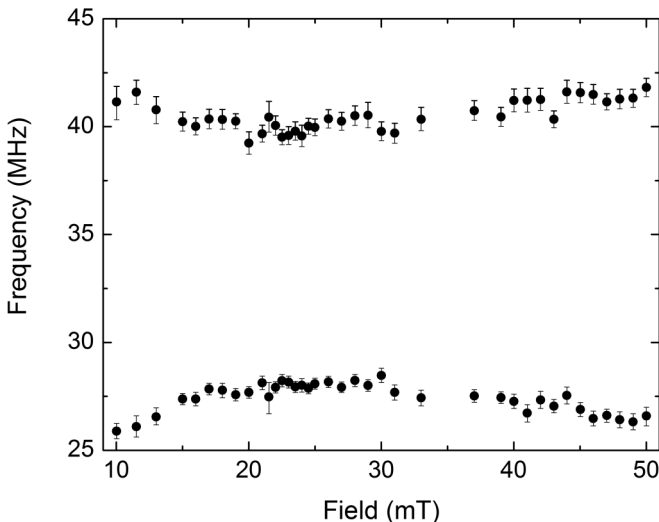


FIG. 6. Magnetic field dependence of the two observed muonium frequencies at  $T = 1.8$  K.

the  $^{19}\text{F}$  spin bath nor the possible broadening of the muon precession linewidth due to the formation of bound  $F\text{-}\mu\text{-F}$  complexes [8] play a significant role in the observed decrease in the muon depolarization rate at the ALC. The muon is responding directly to the magnetic fluctuations of the  $\text{Ho}^{3+}$  ion. This confirms the general utility of transverse field  $\mu\text{SR}$  as a nonresonant technique to probe spin dynamics at avoided level crossings.

To describe spectral and magnetic properties of  $\text{Ho}^{3+}$  ions, we considered the Hamiltonian

$$H = H_{FI} + H_{CF} + H_Z + H_{HFM} + H_{HFQ}, \quad (2)$$

where  $H_{FI}$  is the standard parameterized free-ion Hamiltonian [14],  $H_{CF}$  is the crystal-field interaction,  $H_Z$  is the electronic Zeeman energy,  $H_{HFM}$  and  $H_{HFQ}$  are magnetic and electric quadrupole hyperfine interactions, respectively. Parameters of the free-ion Hamiltonian and crystal-field parameters for  $\text{Ho}^{3+}$  ions in CWO:Ho were presented in Ref. [11]. All calculations mentioned in the present work involved numerical diagonalization of the Hamiltonian  $H_0 = H_{FI} + H_{CF} + H_Z$  operating in the space of 1001 electronic states of the  $4f^{10}$  configuration and subsequent diagonalization of the hyperfine interaction in the truncated basis of 520 electron-nuclear states corresponding to the electronic multiplets  $^5I_J (J = 4 - 8)$ .

From Ref. [11], the important quantitative differences in the energy diagrams of  $\text{Ho}^{3+}$  at sites of tetragonal symmetry in CWO:Ho and LYF:Ho are (a) the  $g$  factor for  $\mathbf{B} \parallel c$ ,  $g_{\parallel}$ , is slightly increased for CWO:Ho (13.7) compared to LYF:Ho (13.3); (b) the gap between the ground state doublet and first excited singlet is larger for CWO:Ho (13 K) than for LYF:Ho (10 K); (c) as a consequence of (b), the tunneling gaps  $\Delta_1$  at the ALCs with  $\Delta I_z = 2$  are reduced in CWO:Ho compared to LYF:Ho (according to calculations,  $\Delta_1 = 220$  MHz in CWO:Ho and 305 MHz in LYF:Ho); and (d) the heterovalent doping required to maintain charge balance in CWO:Ho increases random strains in the crystal lattice relative to LYF:Ho. The increased strain in turn is expected to increase the size of a tunneling gap for an ALC with  $\Delta I_z = 0$  [11], which is also present at the  $n = 1$  field value. Taken in total, none of these will significantly alter the high frequency fluctuations at the ALCs, and this accounts for the close similarity between the transverse field  $\mu\text{SR}$  results for both systems. In contrast to the AC susceptibility data, the ALC near 46 mT ( $n = 2$ ), which has very small tunneling gaps, is suppressed in both LYF:Ho and CWO:Ho when probed with  $\mu\text{SR}$ . Because the change in muon depolarization rate is sensitive to frequencies greater than the muon precession frequency (MHz range), it may be that  $\mu\text{SR}$  probes the adiabatic susceptibility as opposed to the isothermal susceptibility as measured by AC susceptibility in the kHz range. High frequency AC susceptibility measurements, in parallel with a theoretical investigation of the relevant relaxation mechanisms (e.g., phonon and cross-relaxation processes [4,5]) into the MHz range are underway to study this crossover further.

We now look more closely at the DC and AC magnetic measurements (Figs. 1 and 2). The changes in the AC susceptibility are far less dramatic than those reported for LYF:Ho. High-frequency EPR measurements on CWO:Ho

[11] revealed the presence of  $\text{Ho}^{3+}$  ions in four distinct types of low-symmetry sites, in addition to the sites with tetragonal symmetry, which were attributed to the heterovalent doping. The  $\text{Ho}^{3+}$  ions in low-symmetry environments have crystal-field splittings and  $g$  factors that are different than those of the ions at tetragonal sites. Moreover, the degeneracy of the electronic states is completely broken, and these  $\text{Ho}^{3+}$  ions at low temperature are in the singlet state and have only weak-field-induced moments, so they exhibit none of the spin dynamics characteristic of the tetragonal site ions. To estimate the fraction of tetragonal sites, we have made a simple model to extend simulations as presented in Refs. [5,10]. We assume the  $\text{Ho}^{3+}$  ions are located at sites of either tetragonal [11] (subsystem A) or orthorhombic (subsystem B) symmetry. For simplicity, the rhombic crystal-field component affecting ions in the subsystem B was defined by a single parameter  $B_6^6 = 35 \text{ cm}^{-1}$ , and the corresponding term  $H_{\text{rh}} = B_6^6 O_6^6$  ( $O_6^6$  is the Stevens operator) was added to the crystal-field Hamiltonian used earlier in the analysis of the spectral and magnetic properties of the dominant tetragonal centers [11]. This term transforms the splitting of the ground doublet of tetragonal centers into two singlets with a gap of 6.8 K that is close to the average value of the gaps revealed by EPR measurements for low-symmetry centers. The two-site model was then used to fit the magnetization versus field data, as shown in Fig. 1; a diamagnetic contribution from the host crystal is also included. The estimated lower bound for Ho concentration is found to be 0.21%, with approximately equal fractions located at tetragonal and orthorhombic sites. We then fit the real and imaginary components of the AC susceptibility in an extension of the calculations carried out in Refs. [5,10]. While this crude model adequately describes the qualitative results, it clearly under(over) estimates magnitudes of the real(imaginary) components. A more complete model of the AC susceptibility, however, is well beyond the scope of this work. The relevant result for this work is that there is a concentration of approximately 0.1% of  $\text{Ho}^{3+}$  ions in a tetragonal environment, comparable to the 0.17% for the LYF:Ho samples studied in Ref. [8].

We can also estimate the tetragonal center concentration using the measured low temperature depolarization rate  $\lambda_{TF}$  in a transverse magnetic field  $B$  of 20 mT, away from the  $n = 1$  anticrossing. We assume that the muon interacts only with dilute magnetic impurities and that the resulting magnetic disorder is static on the muon timescale. Within this model we can calculate the  $\lambda_{TF}$  [15]. The magnetic moments of  $\text{Ho}^{3+}$  ions at sites with tetragonal symmetry are collinear to the  $c$  axis and induce a local dipolar magnetic field with the components

$$B_{\text{dip},\alpha} = \pm(g_{\parallel}\mu_B/2) \sum (3x_{\alpha z} - r^2\delta_{\alpha z})/r^5 \quad (3)$$

at a muon placed at the center of the Cartesian system of coordinates  $(z\parallel c)$ ; in the low-field limit the  $\text{Ho}^{3+}$  in sites of orthorhombic symmetry are nonmagnetic and do not contribute to the depolarization. Here the sum is taken over  $\text{Ho}^{3+}$  ions with the radius vectors  $\mathbf{r}$  and coordinates  $x_{\alpha}$ . The distribution function for the local dipolar field component  $B_{\text{dip}}$  along the external field considered in the framework of the continuum

approximation can be written as follows [16]:

$$W(B_{\text{dip}}) = \frac{\Gamma}{\pi(B_{\text{dip}}^2 + \Gamma^2)}, \quad (4)$$

where  $\Gamma = 2\pi^2 g_{\parallel}\mu_B n_0 C/9v$  is the distribution width in the case of small concentration  $C$  of magnetic ions (here  $n_0 = 2$  is the number of possible Ho positions in the unit cell with the volume  $v = a^2c/2$ ,  $a = 5.242 \text{ \AA}$  and  $c = 11.372 \text{ \AA}$  are the CWO lattice constants [17]). By averaging a fixed muon contribution into the measured asymmetry  $R \cos[\gamma_{\mu}(B + B_{\text{dip}})t]$  over the distribution (3), we obtain the time-dependent amplitude of the signal at the frequency  $f_{\mu}$

$$R(t) = R \int_{-\infty}^{\infty} \cos(\gamma_{\mu} B_{\text{dip}} t) W(B_{\text{dip}}) dB_{\text{dip}} = R \exp(-\gamma_{\mu} \Gamma t). \quad (5)$$

Note, we neglect here relaxation processes which bring stretched exponential time dependences [5]. Thus, the depolarization rate can be approximated by a rather simple expression

$$\lambda_{TF} = 8\pi^2 \gamma_{\mu} g_{\parallel} \mu_B C/9a^2c. \quad (6)$$

The measured  $\lambda_{TF}$  value of  $0.5 \mu\text{s}^{-1}$  corresponds to the concentration  $C = 0.17\%$  of the tetragonal centers that satisfactorily agrees with the analysis of the magnetization. The corresponding width  $\Gamma$  of the local field distribution equals 5.9 Oe.

#### IV. CONCLUSION

To summarize, we have studied the spin dynamics of  $\text{Ho}^{3+}$  ions imbedded in a single crystal host matrix of  $\text{CaWO}_4$ . Three-quarters of the muons come to rest at interstitial crystal sites and probe the local magnetic field, while the remaining muons form muonium. Ions at sites with the full tetragonal symmetry of the crystal exhibit avoided level crossings, which produce fast fluctuations of local magnetic fields that suppress depolarization of muons precessing in the applied field. Our results confirm that this effect is not reliant on an intermediary spin bath, and so transverse field  $\mu\text{SR}$  is an effective nonresonant probe of magnetic fluctuations at avoided level crossings [8].

#### ACKNOWLEDGMENTS

Muon experiments were performed at the Swiss Muon Source at the Paul Scherrer Institute (Switzerland). Measurements in the MPMS3 system at Boston College were supported in part by NSF Grant No. DMR-1337567. B.Z.M. acknowledges the support by the Russian Foundation for Basic Research Grant No. 17-02-00403. We are grateful to Dr. Alexandra Tkachuk who provided the sample studied in this work.

- [1] L. Thomas, F. Lioni, R. Ballou, D. Gatteschi, R. Sessoli, and B. Barbara, *Nature (London)* **383**, 145 (1996); J. R. Friedman, M. P. Sarachik, J. Tejada, and R. Ziolo, *Phys. Rev. Lett.* **76**, 3830 (1996).
- [2] R. Giraud, W. Wernsdorfer, A. M. Tkachuk, D. Mailly, and B. Barbara, *Phys. Rev. Lett.* **87**, 057203 (2001).
- [3] R. Giraud, A. M. Tkachuk, and B. Barbara, *Phys. Rev. Lett.* **91**, 257204 (2003).
- [4] S. Bertaina, B. Barbara, R. Giraud, B. Z. Malkin, M. V. Vanuyunin, A. I. Pominov, A. L. Stolov, and A. M. Tkachuk, *Phys. Rev. B* **74**, 184421 (2006).
- [5] R. C. Johnson, B. Z. Malkin, J. S. Lord, S. R. Giblin, A. Amato, C. Baines, A. Lascialfari, B. Barbara, and M. J. Graf, *Phys. Rev. B* **86**, 014427 (2012).
- [6] M. J. Graf, A. Lascialfari, F. Borsa, A. M. Tkachuk, and B. Barbara, *Phys. Rev. B* **73**, 024403 (2006).
- [7] B. Z. Malkin, M. V. Vanyunin, M. J. Graf, J. Lago, F. Borsa, A. Lascialfari, A. M. Tkachuk, and B. Barbara, *Eur. Phys. J. B* **66**, 155 (2008).
- [8] M. J. Graf, J. Lago, A. Lascialfari, A. Amato, C. Baines, S. R. Giblin, J. S. Lord, A. M. Tkachuk, and B. Barbara, *Phys. Rev. Lett.* **99**, 267203 (2007).
- [9] G. S. Shakhurov, M. V. Vanyunin, B. Z. Malkin, B. Barbara, R. Yu. Abdulsabirov, and S. L. Korableva, *Appl. Magn. Res.* **28**, 251 (2005).
- [10] R. C. Johnson, K. H. Chen, S. R. Giblin, J. S. Lord, A. Amato, C. Baines, B. Barbara, B. Z. Malkin, and M. J. Graf, *Phys. Rev. B* **83**, 174440 (2011).
- [11] G. S. Shakhurov, E. P. Chukalina, M. N. Popova, B. Z. Malkin, and A. M. Tkachuk, *Phys. Chem. Chem. Phys.* **16**, 24727 (2014).
- [12] A. Yaouanc and P. Dalmas de Réotier, *Muon Spin Rotation, Relaxation, and Resonance: Applications to Condensed Matter* (Oxford University Press, New York, 2011).
- [13] R. F. Kiefl, M. Celio, T. L. Estle, S. R. Kreitzman, G. M. Luke, T. M. Riseman, and E. J. Ansaldo, *Phys. Rev. Lett.* **60**, 224 (1988).
- [14] W. T. Carnall, G. L. Goodman, K. Rajnak, and R. S. Rana, *J. Chem. Phys.* **90**, 3443 (1989).
- [15] See Ref. 12, Section 6.6.2.
- [16] C. Held and M. W. Klein, *Phys. Rev. Lett.* **35**, 1783 (1975).
- [17] D. Errandonea and F. J. Manjón, *Prog. Mater. Sci.* **53**, 711 (2008).